J Electr Eng Technol Vol. 9, No. 6: 2013-2018, 2014
http://dx.doi.org/10.5370/JEET.2014.9.6.2013

ISSN(Print) 1975-0102
ISSN(Online)2093-7423

Measurement and Comparison of Iron Loss in Bonded- and Embossed-Type Segmented Stator Cores for IPMSM

Kwangyoung Jeong*, Dianhai Zhang, Jaehoon Kwon*, Ziyan Ren** and Chang-Seop Koh†**

Abstract – According to the manufacturing process of the laminated stator core for an inserted permanent magnet synchronous motor (IPMSM), the iron loss may be different. It is because the mechanical stress imposed to electrical steel sheet is strongly dependent on the manufacturing process. This paper proposes a new iron loss measurement algorithm which utilizes the induced voltage of a search coil and exciting current. The method is effective even when the distribution of magnetic flux density is not uniform along the magnetic flux path as well as uniform. The developed iron loss measurement system is applied to bonded- and embossed-type segmented stator cores of an IPMSM, and the iron losses are quantitatively compared.

Keywords: Bonded core, Embossed core, Iron loss, Iron loss measurement, Segmented stator core

1. Introduction

Nowadays, most countries are making efforts to increase the energy efficiency of rotating electric machines such as induction motor and permanent magnet motor since normally these machines consume substantial amount of electrical energy [1-4]. The foregoing researches include shape optimal design [1, 2] and employment of better quality of electrical steel sheet (ESS) with more advantageous magnetic properties [4]. Recent researches practically reveal that the manufacturing process of stator core is one of the major factors which deteriorate the magnetic performance of ESS via mechanical stress; in addition, iron loss mostly increases during the laminating process [5, 6]. Nevertheless, until now, we can hardly find any research on the measurement and quantitative comparison of iron losses according to the ways of lamination such as welding, embossing, and bonding.

Fig. 1 shows the structure of bonded- and embossed-type laminated cores, where the embossed-type lamination looks as if it imposes more mechanical stress on the ESS and cause more deterioration of the magnetic properties than the bonded-type one [7]. For this reason, it is believed, in general, that the welded- and embossed-type laminated stator cores have more iron loss than the bonded-type one.

Iron loss inside the ESS, conventionally, is evaluated based on the measurement of magnetic flux density and field intensity under the assumption that they are uniform along the magnetic flux path as in the Epstein frame, the Single Sheet Tester (SST), and the Ring-type specimen method [8, 9]. The stator core of a motor of which segment is shown in Fig. 2. However, it has non-uniform magnetic flux density and field intensity along its magnetic flux path.

Based on the above background, in this paper, a novel iron loss measuring system is developed for a stator core segment with the help of auxiliary yokes to form a magnetic flux path. The developed system evaluates the iron loss based on the measurement of the induced voltage of a B-search coil and exciting current, and is applied to a

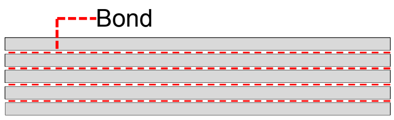

(a) Bonded-type core

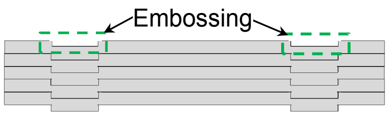

(b) Embossed-type core

Fig. 1. Configuration of laminated core.

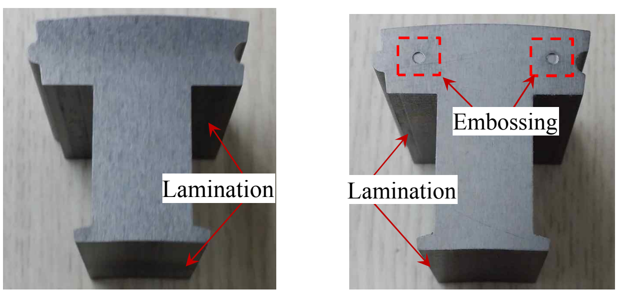

(a) Bonded-type malination (b) Embossed-type malination

Fig. 2. A stator core segment.

† Corresponding Author: College of Electrical and Computer Engineering, Chungbuk National University, Korea. (kohcs@chungbuk.ac.kr)
* College of Electrical and Computer Engineering, Chungbuk National University, Korea. ({cookie7654, renziyan, fivestar88}@chungbuk.ac.kr)
** School of Electrical Engineering, Shenyang University of Technology, China. (renziyan@chungbuk.ac.kr)
Received: April 20, 2014; Accepted: July 10, 2014

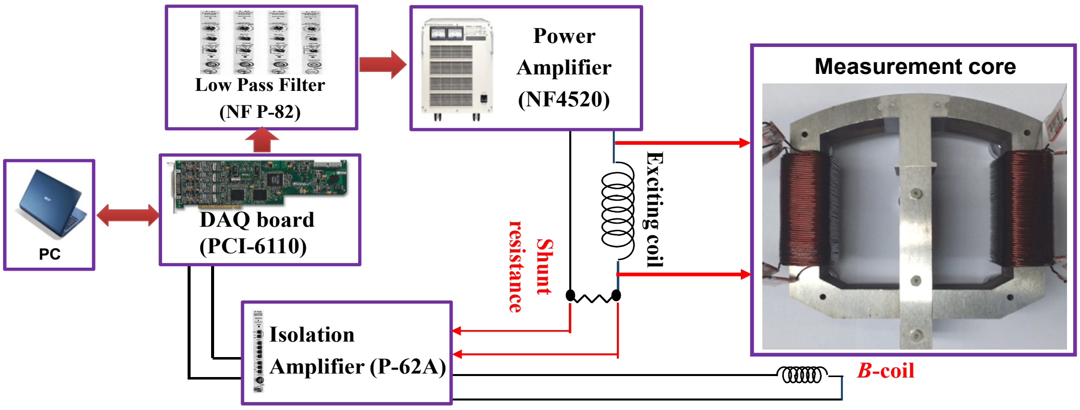

Fig. 3. Measurement system.

bonded- and embossed-type laminated segments of stator core, shown in Fig. 2, for IPMSM.

2. Iron Loss Measurement System

2.1 Measurement system

Fig. 3 shows the configuration of the developed measurement system. It consists of a PC, DAQ board (NI PCI 6110), low pass filter (NF P-82), power amplifier (NF 4520) which is connected to the left and right legs of the auxiliary yoke, respectively, isolation amplifier (NF P-62A), and shunt resistance (0.05 Ω) for measuring the exciting current.

For the measurement of stator core segment, the iron loss is measured with the help of auxiliary yoke, as shown in Fig. 4, in two cases by controlling the exciting voltage waveforms: case 1 is when the magnetic flux passes the tooth part, and case 2 is when there is only return yoke part. In the design of the auxiliary yoke, the width of the central leg (case 1 in Fig. 4) is set equal to the width of tooth and those of the left and right ones that of return yoke of the stator core segment. Therefore, it guarantees almost same magnetic flux density is obtained along magnetic flux path.

On the other hand, for the measurement of 24-segment assembled stator core (case 3 as shown in Fig. 4), iron loss is measured by using the Ring-type method [10], where the exciting coil and *B*-search coil are located at the return yoke.

During the measurement, exciting voltage waveform of exciting coil is controlled using digital feedback method so that the sinusoidal *B*-waveform is obtained at the *B*-search coil. The *B*-search coil is placed between the auxiliary yoke and exciting coil [11]. The measuring frequencies are set to 50 Hz and 400 Hz considering the rotating speed of the IPMSM.

According to measuring frequency, number of turns of exciting coil is set, as shown in Table I, to utilize maximum available power of the power amplifier [10]. Other specifications of different cases are also shown in Table 1.

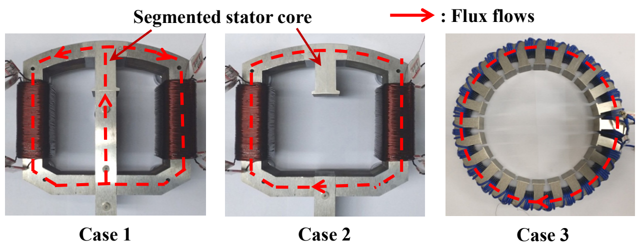

Fig. 4. Measurement cases.

Table 1. Specifications of measuring system

Case	Frequency	No.of exciting coil turns			No.of *B*-search coil turns		
		Left	Right	Connection	Left	Right	Connection
1&2	50 Hz	215	215	Serial	3	3	Serial
	400 Hz	55	55	Parallel	3	3	Serial
3	50 Hz	120 turns			3 turns		
	400 Hz	48 turns			3 turns		

2.2 Iron loss calculation

2.2.1 Conventional method [5]

Conventionally the specific iron loss P_L is calculated, as in the Epstein frame and the SST, as follows:

$$P_L = \frac{1}{\rho T}\int_T \vec{H}(t)\cdot\frac{d\vec{B}(t)}{dt}dt \quad [\text{W/kg}], \tag{1}$$

where B and H are magnetic flux density and magnetic field intensity , respectively; ρ is mass density and T is a time period. In general, the magnetic flux density is measured by using *B*-search coil as follows:

$$B(t) = -\frac{1}{(NA)_B}\int_0^t e(\tau)d\tau \quad [T], \tag{2}$$

where e is the induced voltage of *B*-search coil of which the area turn is $(NA)_B$, and the magnetic field intensity can be measured by using *H*-coil method or Ampere's circuital law by measuring the exciting current [8-10].

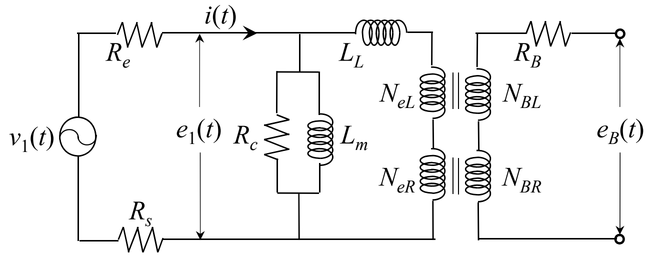

Fig. 5. Equivalent electric circuit of the measuring system, where R_e, R_B are resistances of exciting and *B*-search coils, respectively; R_s is shunt resistance, L_m and L_L are magnetizing and leakage inductances; R_c represents the iron loss resistance; N_{eL} and N_{eR} are the winding turns of exciting coils on left and right legs, respectively; N_{BL} and N_{BR} are winding turns of *B*-search coils on left and right legs, respectively.

It should be noticed that this method is effective only when distributions of *B* and *H* are uniform along flux path.

2.2.2 Proposed method

Fig. 5 shows an equivalent electric circuit of the measuring system, where the iron loss along the magnetic flux path (including the auxiliary yoke) corresponds to the power dissipated at the resistance R_c, and can be calculated as follows:

$$P = \frac{1}{T}\int_T e_1(t)\cdot i(t)\,dt \quad [\mathrm{W}], \tag{3}$$

where the exciting current, *i*(*t*), is measured, as shown in Fig. 5, using a shunt resistor R_s. The voltage $e_1(t)$ is indirectly measured via $e_B(t)$ with the assumption that the leakage inductance is ignorable. The iron loss can be measured as follows:

$$P = \frac{1}{T}\int_T \left\{ \frac{N_{eL}}{N_{BL}} e_{BL}(t) + \frac{N_{eR}}{N_{BR}} e_{BR}(t) \right\} \cdot i(t)\,dt \quad [\mathrm{W}], \tag{4}$$

where $e_{BL}(t)$ and $e_{BR}(t)$ are induced voltages of the *B*-search coils on left and right legs, respectively.

In this method, there exists leakage inductance L_L which may significantly affect on the accuracy of the measurement unless it is ignorable. To resolve this issue, in this paper, *B*-search coils are located under the exciting coil [12]. The measured iron loss in this method is from not only the stator core segment but also the auxiliary yoke [13]. The iron loss from the stator core segment only cannot be separately measured.

3. Experimental Results and Discussions

The segmented stator core is one of twenty-four (24) parts of the whole stator core, which is quite small comparing with the whole stator core. Furthermore, the measurements for case 1 and case 2, shown in Fig. 4, consist of four parts, i.e., the segmented stator core and auxiliary yokes. The auxiliary yoke may cause small air-gaps between the segmented stator core and the auxiliary yoke even though auxiliary yoke is tightly fixed to segmented stator core. As a result, the measurement result for the segmented stator core may be slightly different at each measurement. For this reason, for both the embossed- and bonded-type cores, the iron loss is measured with ten samples and their average value is taken as the final measurement result.

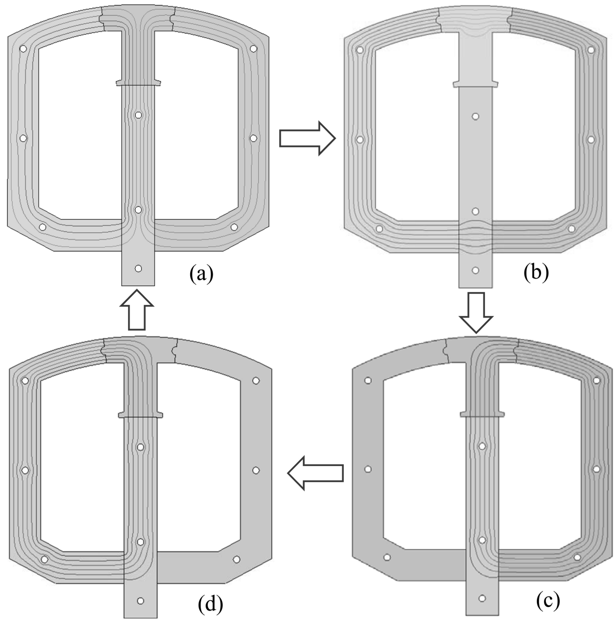

Fig. 6. Flux distribution assumption of real operation of segmented stator core.

When the laminated core segment is assembled into a stator core, it has different distributions of magnetic flux as shown in Fig. 6. The different flux distributions circularly occur under the rotating field condition. Therefore, the combination of iron losses measured from case 1 and case 2 in Fig. 4 can be used to evaluate the iron loss in a segment when it is assembled into an IPMSM operating with a specific rotating speed.

On the other hand, the iron loss measured from the case 3 explains the iron loss from the return yoke of the stator core. This is especially important in the segment-assembled stator cores as the IPMSM in this paper and takes most of the iron loss of the stator core. It is because the tooth of the core segment is, in general, along the rolling direction of the ESS and has *B*-waveform very close to alternating one, thereby very small iron loss while the *B*-waveform at the return yoke is generally similar to rotating one.

Fig. 7 and Fig. 8 show measurement results at frequency of 50 Hz and 400 Hz, respectively. The results for the magnetic flux density of 0.1 T ~ 0.3 T do not have enough

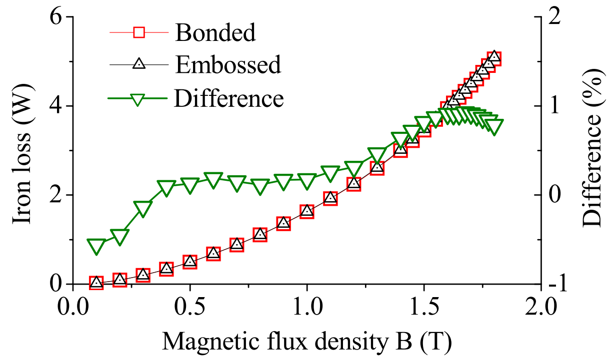

(a) Case 1

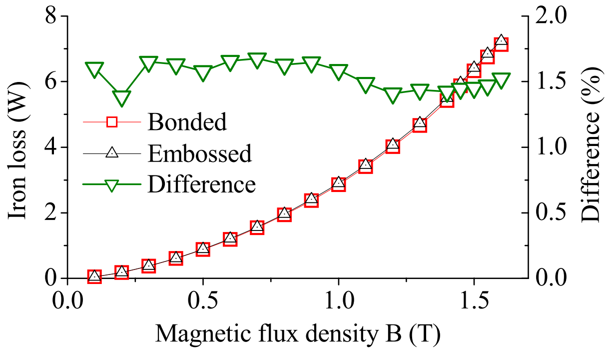

(b) Case 2

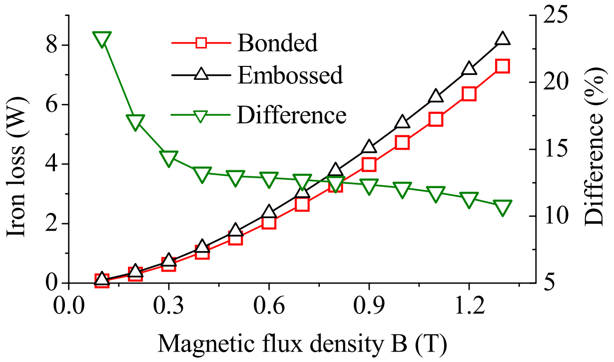

(c) Case 3

Fig. 7. Measurement results at 50 Hz.

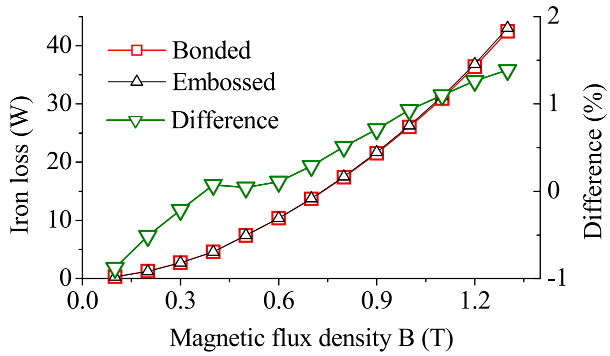

(a) Case 1

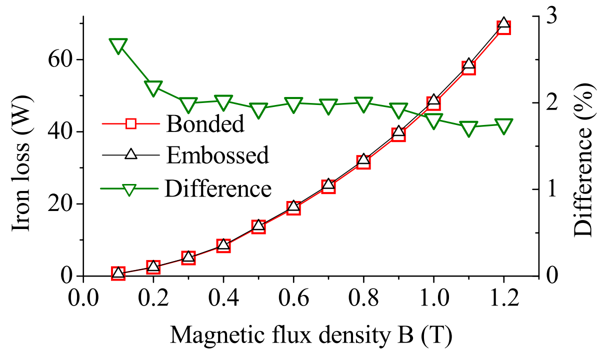

(b) Case 2

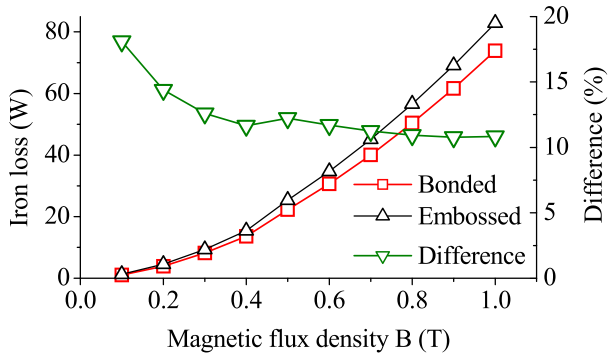

(c) Case 3

Fig. 8. Measurement results at 400 Hz.

physical meaning since the $e_B(t)$ is very small containing a lot of noises.

For the embossed- and bonded- type stator cores in the experiment, the design, thickness of lamination and number of used electrical steel sheets are exactly same. Therefore, to show the difference in the iron loss between the embossed- and bonded-type stator cores, the difference is defined as:

$$\delta = \left(P_E - P_B\right)/P_B \times 100\% \quad (5)$$

where P_E and P_B represent iron losses of embossed and bonded cores, respectively.

It is shown, in Figs. 7 and Fig. 8, that case 2 always gives bigger difference than case 1, for example 1.75% in case 2 and 1.26% in case 1 at the magnetic flux density of 1.2 T under 400 Hz. Considering case 2 is when the magnetic flux passes through embossments while case 1 is not, this reveals that the embossment significantly deteriorates the magnetic properties of the ESS to have more iron loss at the same level of magnetic flux density. It is also shown that the differences become bigger as the measuring frequency increases from 50 Hz to 400 Hz.

When an IPMSM operates, magnetic flux distribution at a core segment will change as shown in Fig. 6. The iron loss at a core segment while motor operation therefore, can be deduced from those measured for cases 1 and 2, i.e., iron loss per segment per period will be approximated to the summation of that from case 2 and twice of that from case 1.

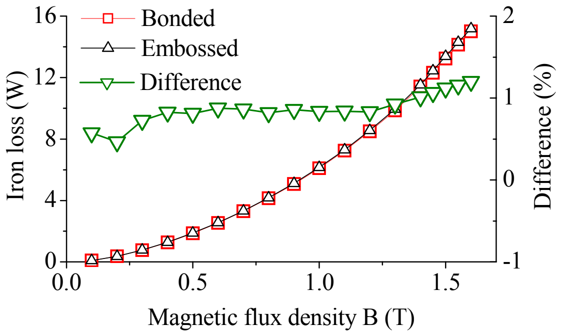

(a) 50 Hz

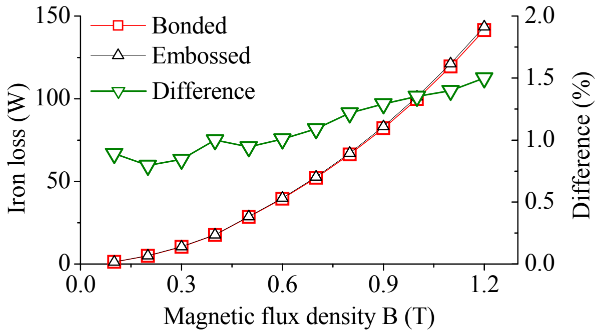

(b) 400 Hz

Fig. 9. Iron loss at the motor operation of assembled stator core.

The corresponding results are shown in Fig. 9, where the difference of iron loss between embossed- and bonded-type core segments is 1.2% at (1.6 T, 50 Hz), and 1.5% at (1.2 T, 400 Hz), respectively.

For measurements of assembled stator core in case 3, the iron loss difference between the bonded- and embossed-type stator cores is about 12.1% at (1.0 T, 50 Hz), and about 10.83% at (1.0 T, 400 Hz). Compared with a segment, this bigger difference comes from the assembled twenty-four (24) cores. It means the bonded-type stator core has less iron loss than the embossed-type one when segments are assembled into an IPMSM.

With the measurement results and iron loss calculation for motor operation, it is obvious that the bonded-type core has less iron loss than the embossed-type core due to smaller mechanical stress during the lamination process.

4. Conclusion

A comparison of iron loss measurement in bonded- and embossed-type segmented stator cores is carried out in this paper. The core segment and segment-assembled stator core are measured to compare the iron losses for a core segment and assembled stator core when lamination is changed from embossment to bonding. From the measurement, it becomes clear that bonding lamination is better than embossment one from the viewpoint of iron loss.

Acknowledgements

This work was supported by the Human Resources Development of the KETEP grant funded by the Korea government Ministry of Knowledge Economy (No. 20104010100600).

References

[1] P-. W. Han, U-. J. Seo, J-. H. Choi, Y-. D. Chun, D-. H. Koo, and J. Lee, "Optimizing design variables for high efficiency induction motor considering cost effect by using genetic algorithm," *Journal of Electrical Engineering and Technology* (*JEET*), vol. 7, no. 6, pp. 948-953, 2012.

[2] D. H. Zhang, C. S. Park, and C. S. Koh, "A new optimal design method of rotor slot of three phase squirrel cage induction motor for NEMA class d speed-torque characteristic using multi-objective optimization algorithm," *IEEE Trans. Magn.*, vol. 48, no. 2, pp. 879-882, Feb. 2012.

[3] G-. W. Cho, C-. M. Kim, and G-. T. Kim, "The maximum efficiency driving in IPMSM by precise estimation of current phase angle," *Journal of Electrical Engineering and Technology (JEET)*, vol. 8, no. 6, pp. 1345-1351, 2013.

[4] M. Takashima, N. Morito, A. Honda, and C. Maeda. "Nonoriented electrical steel sheet with low iron loss for high-efficiency motor cores," *IEEE Trans. Magn.*, vol. 35, no. 1, pp. 557-561, Jan. 1999.

[5] O. Nakazaki, Y. Kai, T. Todaka, and M. Enokizono, "Iron loss properties of a practical rotating machine stator core at each manufacturing stage," *Int. J Appl. Electrom,* vol. 33, pp. 79-86, 2010.

[6] Deepak Singh, "Calorimetric measurement of the stator core losses caused by manufacturing," Master Thesis, AALTO University, Arabia, 2011.

[7] Boglietti A, Cavagnino A, Ferraris L, and Lazzari M, "The annealing influence onto the magnetic and energetic properties in soft magnetic material after punching process," *IEEE Int. Conf. Electric Machines and Drives* (IEMDC'03). vol. 6, pp. 503-508, 2003.

[8] IEC Standard Publication 60404-2, "Methods of measurement of the magnetic properties of electrical steel sheet and strip by means of an Epstein frame," 2008.

[9] JIS C 2556, "Methods of measurement of the magnetic properties of magnetic steel sheet and strip by means of a single sheet tester," 1996.

[10] M. Petkovsek, P. Zajek, J. Nastran, and D. Voncina, "Determination of magnetic properties of soft-magnetic ring cores with a reduced number of primary and secondary winding turns," *IEEE Int. Symp. Ind. Electronics, 2004*, vol. 1, pp. 577-581, 4-7 May 2004.

[11] K. Matsubara, N. Takahashi, K. Fujiwara, and T. Nakata, "Acceleration technique of waveform control for sing sheet tester," *IEEE Trans. Magn.*, vol. 31, no.

6, pp. 2400-2402, Nov. 1995.

[12] K. Y. Jeong, "Measurement of stator core loss of an induction motor at each manufacturing process," Mater Thesis, Chungbuk National University, Korea, 2014.

[13] K. Y. Jeong, Z. Y. Ren, H. S. Yoon, and C-.S. Koh, "Measurement of stator core loss of an induction motor at each manufacturing process," *Journal of Electrical Engineering and Technology* (*JEET*), vol. 9, no. 4, pp. 1309-1314, Jul. 2014.

Kwangyoung Jeong He received his B.S degree in electronic engineering from Hanbat National University, Daejeon, Korea, in 2012, and M.S degree in electrical engineering from Chungbuk National University, Cheongju, Korea, in 2014. He is currently working towards his Ph.D. degree in electrical engineering at Chungbuk National University, Korea. His research interests include the measurement of magnetic properties of electrical steel sheet and the analysis of electromagnetic fields. He can be contacted at cookie7654 @chungbuk.ac.kr.

Dianhai Zhang He received his B.S. and M.S degrees in the biomedical engineering, electrical machine and electric apparatus from Shenyang University of Technology in 2006 and 2009 respectively, and Ph.D degree in electrical engineering from Chungbuk National University in 2013. He is presently a assistant professor at school of electrical engineering, Shenyang University of Technology, China. His research interests include design of electromagnetic devices and numerical analysis of electromagnetic fields. He can be contacted at zdh700@126.com.

JaeHoon Kwon He received his B.S degree in electrical engineering from Chungbuk National University, Cheongju, Korea, in 2013. He is currently working towards his Master degree in electrical engineering at Chungbuk National University, Korea. His research interests include the measurement of magnetic properties of electrical steel sheet and the analysis of electromagnetic fields. He can be contacted at hoy3496@chungbuk.ac.kr.

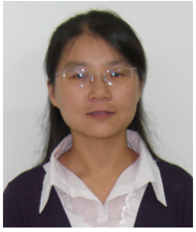

Ziyan Ren She received the B.S degree in biomedical engineering and M.S degree in theory of electrical engineering and new technology from Shenyang University of Technology, China, in 2006 and 2009, respectively. She received the Ph.D degree in Electrical Engineering from Chungbuk National University, Korea, in 2013. She is currently a lecturer in Shenyang University of Technology and Post-doctor in Chungbuk National University. Her research interests include the optimal design of electro-magnetic devices, the numerical analysis of electromagnetic fields. She can be contacted at renziyan@chungbuk.ac.kr.

Chang-Seop Koh He received his B.S., M.S., and Ph. D. degrees in electrical engineering from Seoul National University, Seoul, Korea, in 1982, 1986, and 1992, respectively. He was visiting Professor at the Department of Electrical and Computer Engineering, Florida International University, Florida, USA, and at the Department of Electrical and Computer Engineering, Texas A&M University, Texas, USA, from May 1993 to April 1994, and from February 2003 to January 2004, respectively. He was also a Senior Researcher at the Central Research Institute of Samsung Electro-Mechanics Co., Ltd., from May 1994 to August 1996. He has been a Professor with the College of Electrical and Computer Engineering, Chungbuk National University, Korea, since 1996. His research interests include electric machine design, numerical analysis of electric machines using the finite element. He can be contacted at kohcs@chungbuk.ac.kr.